

Received December 11, 2016, accepted January 15, 2017, date of publication March 8, 2017, date of current version October 12, 2017.

Digital Object Identifier 10.1109/ACCESS.2017.2661967

Incipient Fault Diagnosis of Roller Bearing Using Optimized Wavelet Transform Based Multi-Speed Vibration Signatures

ZHIQIANG HUO^{1,2}, YU ZHANG¹, PIERRE FRANCO³, LEI SHU^{1,2},
AND JIANFENG HUANG², (Member, IEEE)

¹School of Engineering, University of Lincoln, Lincoln LN6 7TS, U.K.

²Guangdong Provincial Key Laboratory on Petrochemical Equipment Fault Diagnosis, Guangdong University of Petrochemical Technology, Maoming 525000, China

³Mines Albi, University of Toulouse, Toulouse 81013 Albi, France

Corresponding author: L. Shu (lei.shu@ieee.org)

This work was supported in part by the National Natural Science Foundation of China under Grant 61401107, in part by the International and Hong Kong, Macao and Taiwan collaborative innovation platform and major international cooperation projects of colleges in Guangdong Province under Grant 2015KGJHZ026, in part by the National Science Foundation of Guangdong Province under Grant 2016A030307029, in part by the Guangdong University of Petrochemical Technology Internal Project under Grant 2012RC106.

ABSTRACT Condition monitoring and incipient fault diagnosis of rolling bearing is of great importance to detect failures and ensure reliable operations in rotating machinery. In this paper, a new multi-speed fault diagnostic approach is presented by using self-adaptive wavelet transform components generated from bearing vibration signals. The proposed approach is capable of discriminating signatures from four conditions of rolling bearing, i.e., normal bearing and three different types of defected bearings on outer race, inner race, and roller separately. Particle swarm optimization and Broyden–Fletcher—Goldfarb–Shanno-based quasi-Newton minimization algorithms are applied to seek optimal parameters of Impulse Modeling-based continuous wavelet transform model. Then, a 3-D feature space of the statistical parameters and a nearest neighbor classifier are, respectively, applied for fault signature extraction and fault classification. Effectiveness of this approach is then evaluated, and the results have achieved an overall accuracy of 100%. Moreover, the generated discriminatory fault signatures are suitable for multi-speed fault data sets. This technique will be further implemented and tested in a real industrial environment.

INDEX TERMS Fault diagnosis, vibration measurement, continuous wavelet transforms, roller bearing, particle swarm optimization, quasi-newton minimization, fault signatures.

I. INTRODUCTION

Roller bearings have been extensively used in industrial environments, where they play a vital role designed for supporting constrained relative rotation and reducing friction between two parts used for transformation of energy. Statistically, the normal service life of a roller bearing is determined by material fatigue, corrosion, and wear at the running surface. Insights into incipient fault detection and diagnosis (FDD) and predictive maintenance are conducive to alleviate the negative impacts of uncertain mechanical failures and proactively provide administrators with the first-time mechanical running state information before severe faults occur. In the last decades incipient FDD of roller bearing has attracted a great deal of attentions attempting to effectively

monitor, diagnose, and isolate bearing faults in purpose of leading to less down-time and economic loss in industrial factories [1].

For several years great efforts has been devoted to the study of fault diagnosis of roller bearing with various condition monitoring methods in terms of vibration signal, acoustic emission, temperature monitoring, and electronic current monitoring [2], [3]. Among those the vibration signals, depicted as machine's signature, particularly enjoy the inherent capability of characterizing typical vibration levels and certain frequency spectrums generated from roller bearings. In practice, vibrations are caused by the transmission of cyclic forces which in fact are behaviors of energy loss. Defective roller bearings therefore gradually generate

various forces causing high amplitude of vibration leading to the increasing energy consumption. For instance, in a specific case of a water pumping station bearing faults would increase vibration level up to 85%, where power consumption increases 14% and pump efficiency decreases 18% [4]. Most importantly, with the advent of accelerometer sensor, collecting data has currently become a simple exercise that helps to provide a wide dynamic range and frequency range for vibration measurement, which has been found to be the most reliable, versatile and accurate.

During the last decades plenty of techniques for FDD of roller bearing have been further studied to establish a firm position based on vibration signal processing. In general, steps of FDD can be mapped into three phrases: data acquisition, feature extraction, and fault classification, and the later two are the priority. The vibration data as initial input is supposed to be correctly operated and measured to reflect equipment's intrinsic behaviors. Feature extraction [5] is regarded as the key step that transforms input data into a reduced set of features which contain critical, compressed, and characteristic information, after which various classification algorithms can be used to map signals into classes of interest, e.g., artificial intelligence. Before that, signal processing techniques are needed to be applied to reduce the magnitude and the redundant information in original signals. Fast Fourier transform (FFT) and short time Fourier transform (STFT) are two approaches for signal decomposition by converting the time domain contents into the frequency spectrum; however, it has been emphasized that it may probably lower down the decomposing performance based on FFT and STFT since inappropriate time windows adopted in these methods [6].

In supplement, a great deal of data-driven models have been further studied to establish a firm position in signal processing. Among those, wavelet analysis is one of the most powerful signal processing techniques which enjoys high resolution in both time and frequency domain [7], [8]. To be more specific, the wavelet analysis has good time and poor frequency resolutions at high frequencies, and good frequency and poor time resolutions at low frequencies. Verifying window size allows the possibility to extract valuable information from vibration signals. Continuous wavelet transform (CWT), one efficient wavelet method, uses groups of non-orthogonal wavelet frames to generate general symptoms, which enjoys the ease of interpretation at the cost of saving space. In addition, with the recent advent of artificial intelligent methods, plenty of techniques have been successfully employed in the field of FDD based on CWT analysis (e.g., artificial neural networks (ANNs), and support vector machine (SVM)). Various artificial intelligence techniques are used with wavelet transform for fault diagnosis in rotating machineries [9], [10], [11]. Zarei *et al.* [12] proposed a method for diagnosis of roller bearings based on ANNs. In this method, vibration signals firstly pass through removing non-bearing fault component (RNFC) filter, and then another neural networks for fault classification. Similarly,

Kankar *et al.* [13] presented an approach for FDD of roller bearings by using three machine learning methods, SVM, ANN, and self-organizing maps (SOM). The results showed that SVM and ANN performed better than SOM. Apart from that, Lou and Loparo [14] introduced a new scheme for the diagnosis of localized bearing defects based on wavelet transform and neuro-fuzzy classification. In [15] a hybrid method based on CWT and SVM was proposed for detecting defects in motor ball bearings.

It is needed to notice that although there are a number of diagnostic approaches have been proposed for bearings based on wavelet analysis, whilst it cannot be neglected that for achieving optimistic accuracy it usually involves a large number of parameters and increasing computation burden. Apart from that, considering of non-stationary and non-linear features commonly exist in vibration signals, the pre-defined kernels may not completely guarantee the convergence to the characteristics of signals. There is still a need to design a new technique that uses optimized wavelet transform directly generated from original signals for multi-speed fault diagnosis of roller bearing in rotating machinery.

In this paper, the impulse modelling based CWT (IMCWT) model is introduced for decomposing vibration signals obtained from roller bearings with wavelet transformation. To obtain optimal IMCWT model, PSO and Broyden-Fletcher-Goldfarb-Shanno (BFGS) based quasi-Newton optimization algorithms are respectively used to optimize IMCWT model for global and local optimization. After that, three-dimensional statistical parameters are applied to extract fault characteristics. Nearest Neighbor (NN) classifier using Mahalanobis distance is adopted to map samples into corresponding categories. Combining IMCWT decomposition, PSO and BFGS-based quasi-Newton optimization algorithms, three-dimensional feature extraction, and NN-based classifier using Mahalanobis distance evaluation a novel intelligent fault diagnostic approach for roller bearings is presented with experimental validation.

The main contributions in this paper are concluded as follows:

- An optimized impulse modelling approach was proposed for wavelet analysis to characterize fault features within vibration signatures obtained from roller bearings.
- In this paper, a hybrid approach for multi-speed fault diagnosis of roller bearing was proposed based on the optimized impulse modelling continuous wavelet transform and statistical analysis with NN-based classifier using Mahalanobis distance.
- Statistical parameters were evaluated and compared by investigating their performances of speed sensitivity and discriminatory potentials to generate fault signatures corresponding to different speeds.
- In experimental results 2D and 3D fault signatures in feature space dimension were generated, meanwhile accuracy of results was verified which has been illustrated that the proposed approach can be effectively

used for generating both single and multi speed fault signatures based on vibration monitoring.

The rest of this paper is organized as follows: Section II introduces IMCWT model and describes parameter optimization method of IMCWT model using PSO and BFGS-based quasi-Newton minimization techniques. Section III presents the proposed fault diagnostic methodology for generating multi-speed fault signatures. Experimental validation, results and multi-speed fault signatures are given in Section IV. Finally, the conclusion of this paper is presented in Section V.

II. PROPOSED IMCWT MODEL

In this section, CWT is first briefly introduced. Afterwards, IMCWT is presented for decomposing the redundant original vibration signals of roller bearing. After that, the process of parameter selection and optimization of IMCWT model based on PSO and BFGS-based quasi-Newton optimization techniques are separately introduced.

A. REVIEW OF WAVELET ANALYSIS

Problems of the time and frequency resolution commonly exist regardless of any transform applied in the process of decomposition. CWT was developed as an alternative approach to FFT and STFT to overcome the resolution problem, which decomposes different segments of the time-domain signal with adjustable window function. The CWT wavelet transform is defined as follows:

$$CWT_x^\psi(\gamma, s) = \Psi_x^\psi(\gamma, s) = \frac{1}{\sqrt{s}} \int x(t) \Psi\left(\frac{t-\gamma}{s}\right) dt. \quad (1)$$

where $x(t)$ is the signal, s is the scale factor, γ is the translation parameter, $\Psi(t)$ is the wavelet transforming function, and it is also called the mother wavelet. The term wavelet represents the window function which has finite length. The term mother wavelet means that time functions transformed to map different segments of the signal are derived from one major function. Similar to the frequency used in STFT, the parameters s and $\Psi(t)$ in the wavelet analysis are respectively used in the transforming operation of dilating and translating time function. To be more specific, large s value corresponds to non-detailed global view, and low s value corresponds to a detailed view of the segment of a signal. Particularly, the factor $\frac{1}{\sqrt{s}}$ is used to ensure energy preservation.

In general, wavelet analysis is one of the most powerful techniques used for signal processing. Having been enjoyed the advantages of reliable and flexible abilities of generating general and fine-grained information extraction, CWT has been extensively proved that can be employed in the field of FDD for analysis of non-stationary and non-linear signals.

B. IMPULSE MODELLING BASED CONTINUOUS WAVELET TRANSFORM (IMCWT)

In practice, the response of the system to the instant δ -impulse in vibrodiagnostics can be represented using a pattern depicted as a response of the

single-degree-of-freedom-system, which can be formulated as follows [16]:

$$f(x) = \alpha e^{-\beta x} \cos(wx + \varphi) \quad (2)$$

where $f(x)$ is the displacement, α is the premier amplitude, w is the resonance frequency, which is the frequency of the system fluctuation without resistance. Taking assumption that at the impulsive start the system was at rest into consideration, Eqs. (2) can be applied as a mother wavelet in CWT, which can be expressed as follows:

$$\Psi(t) = \sin(\alpha t + \beta) e^{-\gamma|t|} \quad (3)$$

For keeping minimum parameters in the mother wavelet, this IMCWT model has three parameters that has the ability of representing a system's working state, which therefore can be employed into FDD of roller bearing. To optimize IMCWT model, global and local optimization techniques are used for parameter selection, which are presented in the following.

C. PARAMETER SELECTION WITH GLOBAL AND LOCAL OPTIMIZATION

1) GLOCAL OPTIMIZATION: PSO

The selection of the parameters, in practical applications, has a great influence on the prediction effect of wavelet analysis. PSO, proposed by Kennedy [17], is a population-based global search algorithm, which was developed to optimize a problem by iteratively improve a candidate solution with regard to a given measure of quality. PSO, different from genetic algorithms, has no crossover and variation instead of using the optimal particle search in the solution space. To be more specific, PSO performs by iteratively using a population (called a swarm) of candidate solutions (called particles) in the search-space. The swarm consists of m numbers of particles, each of which has own velocity $v_{i,j}(t)$, current position $x_{i,j}(t)$, and local best known position $pbest_j(t)$ ($i = 1, 2, \dots, m; j = 1, 2, \dots, n$). Each particle moves towards own best previous position and the best known positions found by other particles $gbest_j(t)$ in the search-space, which is expected to move the swarm toward the best solutions. The standard PSO can be performed according to the following equations:

$$v_{i,j}(t+1) = w \times v_{i,j}(t) + c_1 \times r1() \times (pbest_j(t) - x_{i,j}(t)) + c_2 \times r2() \times (gbest_j(t) - x_{i,j}(t)) \quad (4)$$

$$x_{i,j}(t+1) = x_{i,j}(t) + v_{i,j}(t+1) \quad (5)$$

where j is the n th dimension of a particle ($1 \leq j \leq n$), the velocity is restricted to the $[-v_{max}, v_{max}]$ range, $r1()$ and $r2()$ are random numbers in the range of $[0,1]$, c_1 and c_2 are positive constants corresponding to personal and social learning factors, and w is the inertia weight. In this paper, the initialize parameters with respect to the size of swarm, inertia weight, maximum number of iterations are selected as follows: swarm size $p = 20$, $c_1 = 1.3$, $c_2 = 1.75$, max stall iterations $t_{max} = 6$. The search range of α , β , γ is from $[0, 0, 0]$ to $[200, 200, 200]$.

2) LOCAL OPTIMIZATION: BFGS BASED QUASI-NEWTON MINIMIZATION

After generally searching optimized parameters by using global optimization, the the BFGS-based quasi-Newton unconstrained minimization method is used to accurately locate minimum solutions for IMCWT model [18]. In local unconstrained minimization, the quasi-Newton method is one of the most favored optimization methods that uses curvature information at each iteration to formulate a quadratic model problem, which has the following form:

$$\min_{x \in R^n} f(x) = \frac{1}{2}x^T Hx + b^T x + c \quad (6)$$

where H , the Hessian matrix, is a positive definite symmetric matrix, b is a constant vector, and c is a constant. This method has optimal solution when the partial derivatives of x approach to zero shown as below:

$$\nabla f(x^*) = Hx^* + c = 0 \quad (7)$$

The optimal solution, x^* , can be formulated as

$$x^* = -H^{-1}c \quad (8)$$

Different from Newton-type methods that directly calculate H , quasi-Newton methods use the observed behavior of $f(x)$ and its gradient to build up curvature information to properly update an approximation to H , which avoid a large amount of calculation. For Hessian updating, the BFGS is generally thought to be an effective method that can be used for iteratively optimizing the search direction. It's needed to notice that, in BFGS method, H is a positive definite matrix that generates a direction of descent, as a result of which for any small length of step the value of objective function decreases all the time. In BFGS, the formula for generating an approximation to H is described below:

$$H_{k+1} = H_k + \frac{q_k q_k^T}{q_k^T s_k} - \frac{H_k s_k s_k^T H_k^T}{s_k^T H_k s_k} \quad (9)$$

where s_k and q_k are formulated as following:

$$s_k = x_{k+1} - x_k \quad (10)$$

$$q_k = \nabla f(x_{k+1}) - \nabla f(x_k) \quad (11)$$

At the beginning of iterations, H_0 can be set to identify matrix I_0 . This formula therefore can be used to make an approximation of the H^{-1} at each update to avoid a great deal of calculation. After that, line-search method is applied to locate the best solution, x_k , along the search direction by repeatedly minimizing polynomial interpolation models of the objective function. That it, the next iterate x_{k+1} has the following form:

$$x_{k+1} = x_k + \alpha^* d_k \quad (12)$$

where x_k is the current iterate, d_k is the search direction, and α^* is a scalar step length parameter. At each iteration, a line search is performed to locate the best solution in the given direction:

$$d_k = -H_k^{-1} \cdot \nabla f(x_k) \quad (13)$$

In this paper, BFGS based quasi-Newton unconstrained minimization serves to locate optimized parameters after global optimization. The max number of iterations, t_{max} , is set to 80, max number of function evaluations is 300.

3) THE PROCESS OF PARAMETER SELECTION USING GLOBAL AND LOCAL OPTIMIZATION

In this study, for obtaining optimized IMCWT model, there are in total three parameters, namely α, β, γ needed to be evaluated. The process of parameter selection and evaluation with PSO and BFGS based quasi-Newton algorithms is presented in Fig. 1, which is described below:

Step 1: initialization of global optimization. Randomly generate the initial position (corresponding to α, β , and γ) and velocity of each particle. Set the size of swarm, iteration variable $t = 0$, maximum iteration number t_{max} , inertia weight $c1, c2$. Afterwards, start global training process from step 2 to 4.

Step 2: fitness evaluation. The fitness function is designed for evaluating current particles' performance, which is needed to be given before the start of optimization. In this paper trust rate is adopted to evaluate statistical similarity between the new sample and given classes, which is as follows:

$$T_{trust}^i = \left(1 - \frac{d_i}{d_{min} + d_i}\right) \times 100\% \quad (i \in c) \quad (14)$$

where i is the i th number of classes, d_i is the distance between i th class and the new sample. Particularly, since there are only four given fault types studied in this paper, the trust rate of the class with minimum distance can be achieved by using $100 - \max(T_{trust}^i)$. Afterwards, on the basis of trust rate evaluation, fitness function is formulated as below:

$$F_{fit} = -\bar{T}_{trust} = -\frac{\sum_{i=1}^c T_{trust}^i}{c} \quad (15)$$

where c is the total number of classes, \bar{T}_{trust} is the mean trust rate of c kinds of classes. From the above definition, it can be easily seen that the fitness decreases when trust rate increases. It is needed to notice that both PSO and quasi-Newton optimization manners are minimization methods, the fitness value is supposed to decrease with higher classification accuracy. That is, the value of fitness tends to approach to desired solution when the mean similarity increasingly rises between the new sample and four classes.

Step 3: particle update. Update the velocity and position of each particle according to Eqs. (4) and (5).

Step 4: global optimization status checking. If stopping criteria is satisfied, go to step 5. Otherwise, set iteration variable: $t = t + 1$, go to step 2.

Step 5: end global optimization. Finish global optimization, and output global optimized parameters, after which these parameters are to be used as initial parameters to start local optimization in step 6.

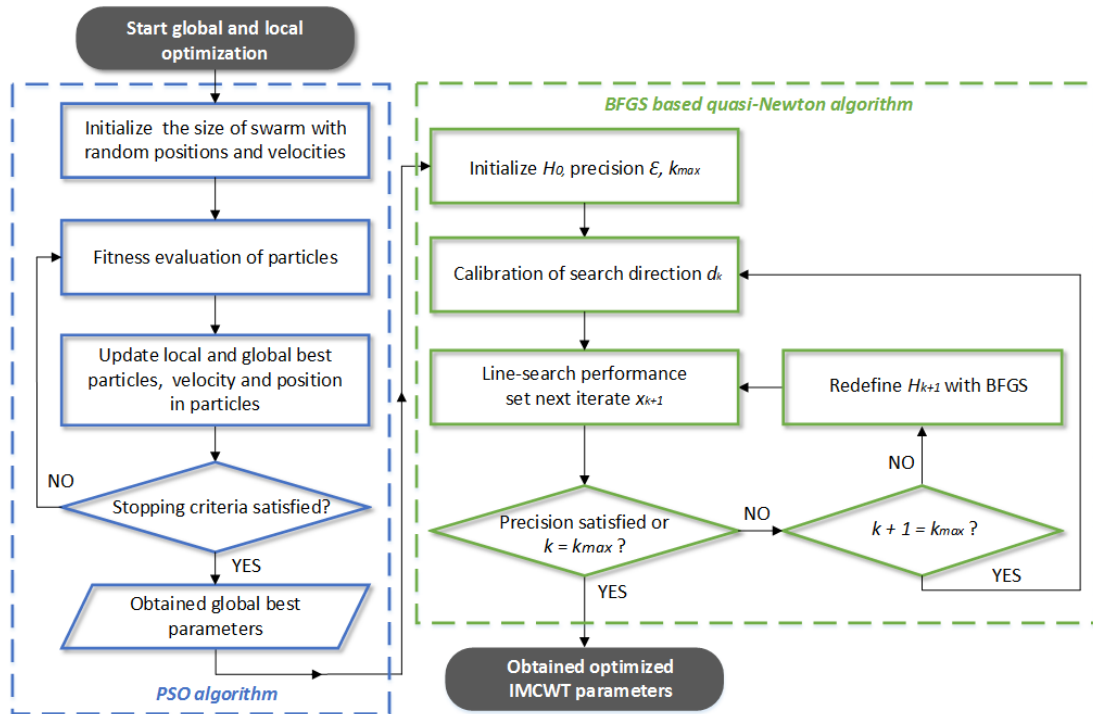


FIGURE 1. The process of parameter selection for IMCWT model using PSO and BFGS-based quasi-Newton optimization.

Step 6: initialization of local optimization. Set up initial points x_0 (i.e., α , β , and γ obtained from PSO), initial matrix $H_0 = I_0$, iteration variable $k = 0$, max iteration number k_{max} , and then perform the training process from step 7 -10.

Step 7: calibration of search direction. Initialize direction d_k corresponding to Eqs. (13).

Step 8: line-search performance. At each step of this performance, the line-search method searches the best solution (containing the current point, x_k) paralleling to current search direction according to Eqs. (12).

Step 9: local optimization status checking. To evaluate the minimum desired value, F_{fit} is applied according to Eqs. (14) and (15). If precision satisfied, go to step 11. Otherwise, judge the current value of k whether meets the value of k_{max} . If next iteration $k + 1 = k_{max}$, go to step 7, and set $x_0 = x_{k_{max}}$. Otherwise, go to step 10.

Step 10: Hessian updating with BFGS. Update positive definite symmetric matrix H_{k+1} and search direction d_{k+1} according to Eqs. (9) - (13), and then go to step 7.

Step 11: end local optimization. Finish the overall training procedure and output the optimized parameters, namely α , β , and γ after global and local optimizations.

III. PROPOSED METHODOLOGY FOR FDD

In general, statistical signal analysis of FDD after signal processing can be mapped into three key phrases: (1) feature extraction; (2) fault classification; (3) fault identification. In this section, the proposed methodology for FDD of roller

bearing is presented, including feature selection of statistical parameters, fault classification, and fault identification.

A. FEATURE SELECTION OF STATISTICAL PARAMETERS

In practical, time-domain statistical parameters have been successfully adopted as trend parameters attempting to reflect the different amplitude and distribution of the time-domain signals, by which an enormous amount of information can be obtained from vibration signals. In this paper, before the step of feature extraction using determined features, the widely used time-domain statistical parameters are applied, each performance of which is investigated for extracting features from wavelet coefficients and generating fault signatures in feature space dimension (i.e., the peak value, root mean square (RMS), crest factor, kurtosis, clearance factor, impulse factor, shape factor, and skewness [19]). Apart from that, wavelet power spectrum density (PSD) is also analyzed, which is used for determining the distribution of energy by computing the absolute-value squared of wavelet coefficients. In addition, rotating speed is considered one of the most critical parameters that has great influences on the performance of statistical parameters. In this study, for obtaining reduced and appropriate parameters for feature extraction and the generation of multi-speed fault signatures, two capabilities of parameters were evaluated, namely speed sensitivity and discriminatory potentials. Obviously for generating discriminatory fault signatures, parameters with low speed sensitivity and high discriminatory ability can be considered as proper indicators for the purpose of distinguishing fault

symptoms in high efficiency. For this purpose, the objective functions used are the values of statistical parameters. Hence, the effect of different speeds on 9 statistical parameters above mentioned is firstly evaluated. In this step, standard deviation and liner normalization are used to make the comparison of the performance of 9 feature candidates when they are applied to discriminate fault symptoms after wavelet decomposition under different speeds. Furthermore, for generating fault signatures, the larger deviation between parameters' values can be considered that has better performance to visually distinguish four conditions of roller bearing. In this paper, the normalized mean value of 9 candidates was primarily computed to analyze the discriminatory ability under different speeds, the experimental result of which is presented in Section IV. After that, desired parameters are selected as proper features which would be later used for representing vibration signals and generating multi-fault signatures. After evaluation, in this paper, reduced three-dimensional feature space dimension is finally adopted, namely RMS [20], kurtosis [21], [22], and PSD [23], which have relatively better discriminatory performance for effectively generating 2D and 3D fault signatures.

$$RMS = \sqrt{\frac{1}{N} \sum_{i=1}^N (x(i) - \bar{x})^2} \quad (16)$$

$$kurtosis = \frac{\frac{1}{N} \sum_{i=1}^N (x(i) - \bar{x})^4}{RMS^4} \quad (17)$$

$$PSD = \sum_{i=1}^N |x(i)|^2 \quad (18)$$

where $x(i)$ is the i th number of wavelet coefficients ($i = 1, 2, \dots, N$), \bar{x} denotes the mean value of the coefficient data points. In this study, RMS and PSD are used to generate single-speed fault signatures for roller bearing with four conditions in 2D feature space dimension. PSD, RMS, and kurtosis are together adopted to produce multi-speed fault signatures in 3D feature space dimension.

B. FAULT CLASSIFICATION

Taking different conditions of roller bearing into consideration, the classification of this kind of fault is multi-class classification problem. NN algorithm is one of the most fundamental and commonly used methods for classification [24], which enables to consistently achieve high performance. The basic idea behind NN method is that a new sample can be classified by calculating the distance as well as similarity between this new sample and given classes, after which the group label of this sample can be determined using a class with the nearest vector distance between this sample. To be more specific, the minimum distance between a undetermined sample and a class may have the greatest similarity compared with other classes. On this basis, a NN-based classification using Mahalanobis distance is therefore adopted in this study for fault classification by mapping new samples into the best matching classes in both training and testing phrases [25].

Suppose that training data set has c classes of feature sets, w_1, w_2, \dots, w_t is $\{p_t^{i,k}, t = 1, 2, \dots, c; i = 1, 2, \dots, N_t; k = 1, 2, \dots, m\}$, where feature set w_t is the t th class in input data, $p_t^{i,k}$ is the i th row in feature set w_t and the k th feature in this row, m is the sum of samples in each row, i corresponding to N_t , N_t is the row number of w_t , which means for each class of bearing, w_t , has in total N_t number of rows. Suppose each feature set w_t has Sum_t number of samples in total.

The major process of multi-fault classification is described as follows:

step 1: In training step, calculate the average feature set in w_t , namely the mean value of each parameter in feature vector t , can be defined below:

$$\bar{w}_t = \frac{\sum_{k=1}^m \sum_{i=1}^{N_t} p_t^{(i,k)}}{Sum_t} \quad (19)$$

step 2: calculate the distance between a new sample s and each average feature set \bar{w}_t using Mahalanobis distance.

$$d_t = \sqrt{(s - \bar{w}_t)S^{-1}(s - \bar{w}_t)^T} \quad (20)$$

where S^{-1} is covariance matrix resulted from s and \bar{w}_t .

step 3: locate the minimum distance d_{min} between sample s and \bar{w}_t , and then perform fitness evaluation corresponding to Eqs. (14) and (15). After that, the category label of this sample can be determined using a class having the minimum fitness value, which means high trust rate and low classification error. It is needed to note that step 1 only needs to be computed once in training phrase to decide the vector center of each class. During testing phrase, only step 2 - 3 are needed to compute the Mahalanobis distance and carry out classification. Additionally, in testing phrase, classification accuracy criteria is applied which can be defined as follows:

$$E_A = \left(\frac{N_f}{N_t + N_f} \right) \times 100\% \quad (21)$$

where N_t and N_f respectively denote the number of true and false classification samples. The classification result with low classification error produces high accuracy approaching to 100%.

C. FAULT IDENTIFICATION

The aggressive adoption of techniques of machine condition monitoring and pattern recognition has helped in laying the foundation for incipient FDD of roller bearing. The main phrases involved in fault detection and identification include: data acquisition, signal analysis, and fault identification. To be more specific, data acquisition is used to collect physical signals of interest to be analyzed, which is supposed to be correctly operated and measured. Signal analysis is commonly composed of data preprocessing, signal processing, and feature extraction. Fault identification generally includes

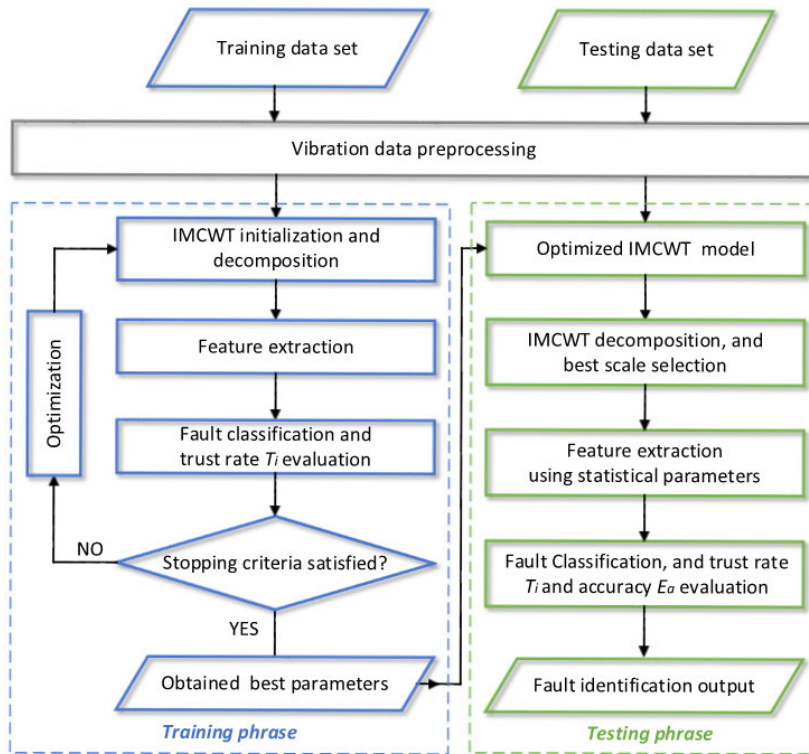


FIGURE 2. Training and testing process of fault diagnosis for roller bearing using proposed techniques.

feature evaluation, and fault classification. Combining statistical techniques, both of these steps have respective advantages and great influences on the fault diagnosis of rotating components in industrial factories.

In this paper, a novel hybrid diagnostic approach for defects detection in roller bearings is proposed based on wavelet analysis, reduced three-dimensional feature extraction, statistical similarity analysis. Optimized IMCWT is obtained by using PSO and quasi-Newton minimization techniques, and then used to decompose vibration signals obtained from roller bearings. Afterwards, three features, namely PSD, RMS, and kurtosis, are applied for characterizing fault symptoms in wavelet coefficients. After that, NN-based classifier using Mahalanobis distance is adopted for fault classification. On the basis of these techniques, the bearing fault diagnostic diagram is formed as illustrated in Fig. 2, the process is described as follows:

Step 1: collect vibration signals of roller bearing by using experimental test rig, and then split data into two data sets to respectively prepare training data set and testing data set.

Step 2: signals are normalized to make the signals comparable regardless of differences in magnitude using the following equation:

$$X_i = \frac{x - \bar{x}}{\sigma} \quad (22)$$

where x is the i th element of the signal, \bar{x} and σ are the mean and standard deviation of the vector respectively.

Step 3: initialize three parameters (α , β , and γ) in CWT transformation using impulse model.

Step 4: perform feature extraction using statistical parameters, in this paper, kurtosis, RMS, and PSD are used for this purpose.

Step 5: classify samples into classes by using NN-based classification method with Mahalanobis distance, and then perform fitness evaluation, F_{fit} , between four given classes and the new sample corresponding to Eqs. (14) and (15).

Step 6: go to global and local optimization algorithm. In this phrase, IMCWT model can be used to perform wavelet analysis with three optimized parameters, before which trust rate evaluation is used to select the best wavelet order according to Eqs. (15). Combining optimized IMCWT model, step 3 - 5 can be used for testing classification accuracy based on this approach by using testing data sets. After that, if results can achieve high accuracy this proposed approach can be used for either off-line or on-line fault diagnosis of roller bearing based on optimized IMCWT model.

IV. EXPERIMENTAL STUDY

In this section, to illustrate the effectiveness of the proposed approach, the fault diagnosis of roller bearing is studied and verified by using experimental test rig. Primarily, comparison

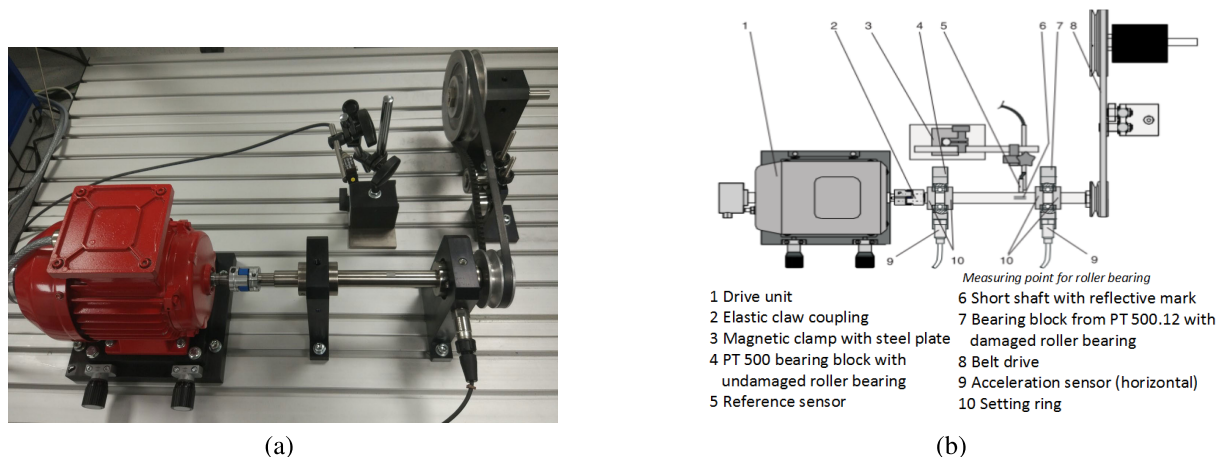


FIGURE 3. PT 500 experimental test rig and corresponding layout graph. (a) PT 500 test rig. (b) layout graph of test rig [26].



FIGURE 4. Four conditions of the experimental bearings. (a) Normal bearing A as reference. (b) Bearing B with outer race defect. (c) Bearing C with inner race defect. (d) Bearing D with roller defect.

study is carried out for evaluating the different performance of statistical parameters and vector distances, which are critical for generating discriminatory multi-speed fault signatures. Afterwards, the experimental results of roller bearing diagnosis and the generation of fault signatures are investigated and presented using the proposed approach in this paper.

A. EXPERIMENTAL SYSTEM DESCRIPTION

In this study, PT 500 machinery diagnostic system [26] is used to collect vibration signals of four conditions of roller bearing, as shown in Fig. 3 (a) and (b). Roller bearing faults kit is composed of motor assembly, motor control unit, shaft, four types of bearings, belt drive kit, and computerised vibration analyser. The control unit is used to collect speed and horsepower data. The piezo-electric sensor and measurement amplifier are used for acceleration measurement. During the tests, vibration data were captured at a sampling frequency of 8 kHz for different bearing conditions. Roller bearings used in this paper are illustrated in Fig. 4, which are bearing A without damage, bearing B with outer race damage, bearing C with inner race damage, and bearing D with rolling element damage. To study and evaluate the performance of the proposed approach, four conditions of roller bearing were monitored and respectively recorded under five rotating speeds. That is, 1000, 1500, 2000, 2500 and 3000 r.p.m.

The experimental data set contains four conditions of roller bearing, for each condition in one speed, 200 data sets are used, and therefore the total number of data set corresponding to four roller bearings is 800. In each of data set 4096 sampling points are used. Finally, the entire data set is split into two data sets, namely 400 for training and 400 for testing respectively.

B. EXPERIMENTAL RESULTS

1) ANALYSIS OF STATISTICAL PARAMETERS AND DISTANCE FUNCTION FOR FAULT DIAGNOSIS

In this paper, before determining reduced three-dimensional features, widely used statistical parameters were firstly analyzed to select proper candidates with high discriminatory ability and performance which would be applied to generate multi-speed fault signatures. For this purpose, in total 9 statistical parameters were primarily investigated to extract fault symptoms under two rotating speeds, 500 and 3000 r.p.m respectively. These 9 parameters are represented from x_1, x_2, \dots, x_9 , including shape factor, kurtosis, PSD, RMS, peak, crest factor, clearance factor, skewness factor, and impulse factor. In this study, considering four conditions of roller bearing and two speeds, there are in total 1600 data sets were used to compare their performance. The second-scale Morlet wavelet was chosen for the application of wavelet

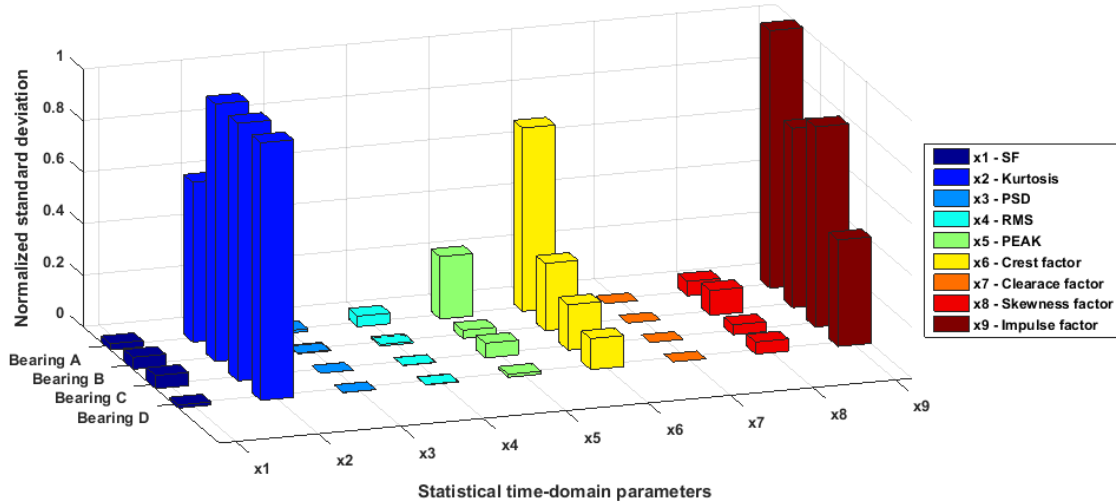


FIGURE 5. The deviation of statistical parameter values under different speeds (i.e., 500 and 3000 r.p.m) using linear normalization.

TABLE 1. The comparative results of vector distance using three speed data sets: 1000, 2000, and 3000 r.p.m.

Vector distance	Bearing A Trust rate(%)	Bearing B Trust rate(%)	Bearing C Trust rate(%)	Bearing D Trust rate(%)	Mean trust rate (%)	Testing accuracies (%)
Mahalanobis	99.15	86.46	96.69	95.48	94.45	100
Euclidean	98.94	84.29	91.10	95.36	92.42	100
CityBlock	99.16	77.79	94.61	95.86	91.86	100
Chebyshev	97.35	91.77	80.00	92.48	90.40	100

TABLE 2. Single-speed resulting trust rate of fault detection and identification on roller bearing.

Single speed	Bearing A Trust rate(%)	Bearing B Trust rate(%)	Bearing C Trust rate(%)	Bearing D Trust rate(%)	Mean trust rate (%)	Testing accuracies (%)
1000	99.77	98.36	96.17	99.74	98.52	100
1500	99.75	99.44	98.40	99.79	99.35	100
2000	99.75	99.46	99.44	98.50	99.28	100
2500	99.85	99.92	99.58	99.66	99.75	100
3000	99.70	97.47	80.00	98.58	97.03	100

transform, after which statistical parameters were used to extract features, and then standard deviation was applied to evaluate the dispersion degree of each parameter in same bearing condition and speed. From Fig. 5, it can be concluded that kurtosis, crest factor, and impulse factor are the most sensitive parameters for detecting incipient faults corresponding to increasing speeds. For the purpose of generating multi-speed fault signatures, sensitive parameters however are not the proper candidates since the mean value of which would increasingly change following with the increasing speed, as a result of which these parameters may be probably too sparse to represent one sample in feature space dimension. Less sensitive parameters therefore are chosen in this study, among

those shape factor, PSD, RMS, and clearance factor are both considered as appropriate candidates to draw fault signatures. It is needed to note that both of these parameters perform well in feature extraction, in this study only reduced three-dimensional feature space dimension is considered for fault feature extraction and generation of fault signatures. That is, each coefficient after wavelet decomposition is represented by its three-dimensional feature vector.

Additionally, the ability of discriminatory potential of each statistical parameter was evaluated by making comparison between mean values of statistical parameters when used to achieve better separability representing four bearing conditions. Four rotating speeds (i.e., 1500, 2000, 2500 and

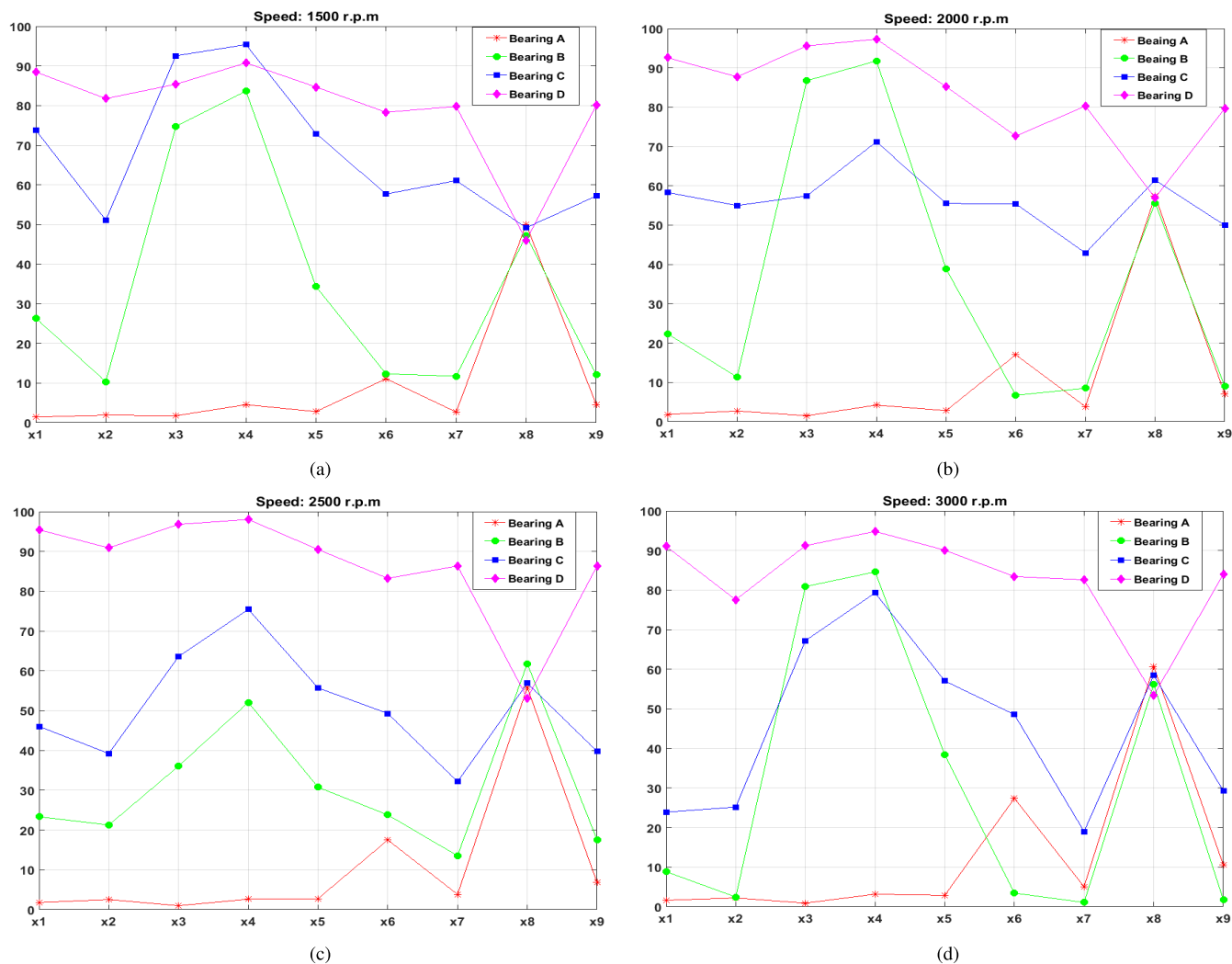


FIGURE 6. The discriminatory ability of statistical parameters representing roller bearings under various rotating speed. (a) Mean value of statistical parameters with 1500 r.p.m. (b) Mean value of statistical parameters with 2000 r.p.m. (c) Mean value of statistical parameters with 2500 r.p.m. (d) Mean value of statistical parameters with 3000 r.p.m.

TABLE 3. Multi-speed resulting trust rate of fault detection and identification on roller bearing.

The number of speed	Speeds	The number of training data sets	The number of testing data sets	The number of misclassified data sets	Trust rate	Testing Accuracies(%)
1	1000	400	400	0	98.94	100
2	1000,1500	800	800	0	98.38	100
3	1000,1500,2000	1200	1200	0	94.45	100
4	1000,1500,2000,2500	1600	1600	0	91.77	100
5	1000,1500,2000,2500,3000	2000	2000	0	91.10	100

3000 r.p.m) and in total 3200 data sets were tested in this study, the result of which is illustrated in Fig. 6. From this figure, it can be seen that parameters in the left side can relatively discriminate four bearing conditions after normalization from 0 to 100. To be more specific, four bearing conditions can be separately represented by one parameter

with different values after normalization. Hence, comprehensively taking speed sensitivity and discriminatory potential into account, in this proposed study, PSD, RMS are selected as features to generate 2D fault signatures. Moreover, it can be seen from Fig. 5 that kurtosis is highly sensitive to variation of rotating speed, which is an appropriate feature

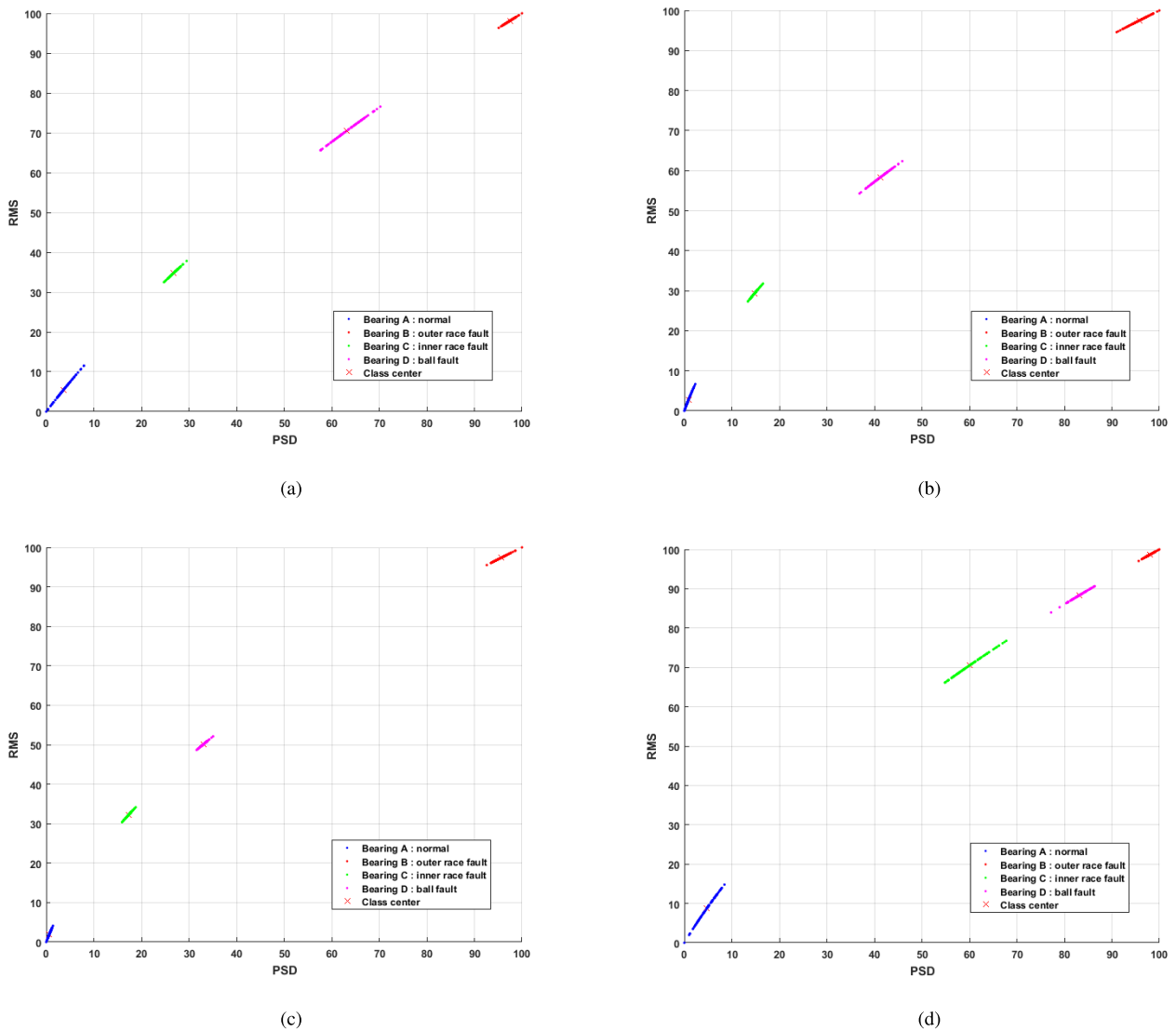


FIGURE 7. The 2D fault signatures with single-speed showing training data distribution for fault diagnosis. (a) Fault signatures distribution with 1000 r.p.m. (b) Fault signatures distribution with 1500 r.p.m. (c) Fault signatures distribution with 2500 r.p.m. (d) Fault signatures distribution with 3000 r.p.m.

TABLE 4. Classification accuracy comparison by using CWT with different kernels under five different speeds.

Operating wavelet	The number of resolution level	The number of testing data sets	The number of misclassified	Trust rate (%)	Testing accuracies (%)
IMCWT	4	2000	0	94.60	100
Daubechies2	3	2000	0	90.45	100
Daubechies4	3	2000	0	89.79	100
Daubechies10	3	2000	0	87.57	100
Mexican hat	1	2000	3	87.23	99.85
Haar	3	2000	6	88.39	99.72
Meyer	3	2000	28	70.22	98.60
Morlet	3	2000	42	83.41	97.90

that can be used to transfer 2D feature space to 3D dimension when multi-speed signals involved for fault diagnosis. Therefore, combining kurtosis, RMS, and PSD together this

three-dimensional feature space can be properly applied to generate multi-speed fault signatures in 3D feature space dimension. In addition, to illustrate the selected

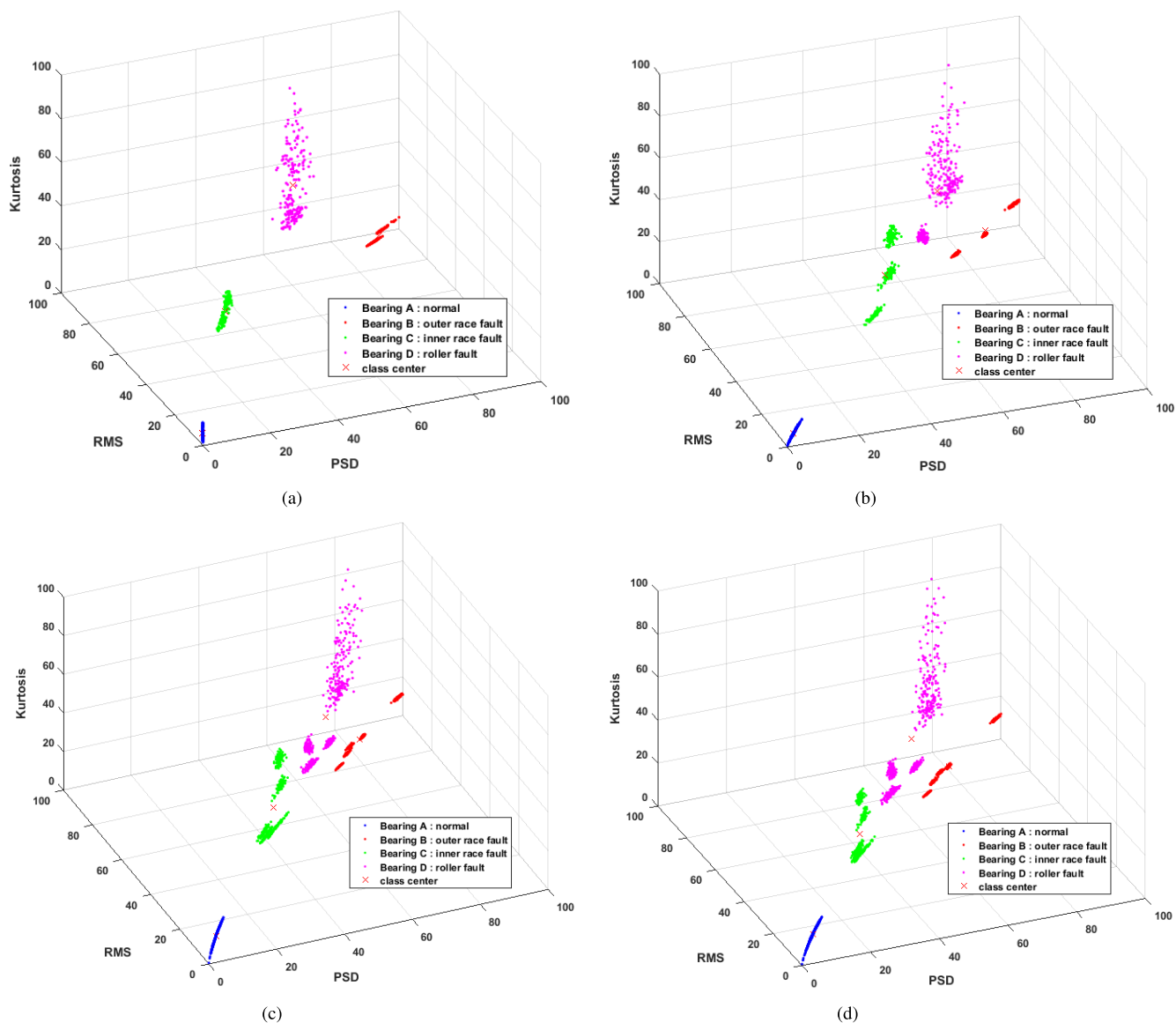


FIGURE 8. (a) Fault signatures distribution with 1000, and 1500 r.p.m. (b) Fault signatures distribution with 1000, 1500, and 2000 r.p.m. (c) Fault signatures distribution with 1000, 1500, 2000, and 2500 r.p.m. (d) Fault signatures distribution with 1000, 1500, 2000, 2500, and 3000 r.p.m.

distance function, Mahalanobis, has better performance in NN-based classification, commonly used vector distances (i.e., Euclidean, City Block, Chebyshev) were selected to evaluate similarity between the new sample and given classes. Trust rate and classification accuracy were applied to evaluate the classification results corresponding to Eqs. (14) and (19). As shown in Table I, it can be seen that both of four distances can achieve 100% accuracy. Mahalanobis analysis however achieved more high trust rate than the rest. That is, the mean similarity between correct classification and samples evaluated by Mahalanobis distance is more relatively accurate than the others. According to the literatures, different from other similarity distances, Mahalanobis distance takes the correlations of data sets into account. Hence, Mahalanobis distance used for statistical similarity analysis is more unitless and scale-invariant.

2) EXPERIMENTAL RESULTS OF MULTI-SPEED FAULT DIAGNOSIS AND SIGNATURES

After having determined the feature vector and vector distance method, original vibration data sets of roller bearing were used to verify the effectiveness of this proposed approach and multi-speed fault signatures. Primarily, the classification accuracy of single-speed diagnosis and the fault signatures are illustrated in Fig. 7 and Table II. Fig. 7 shows the 2D data distribution plots of the samples under a single speed in this study. It can be noticed that the training data sets with fault symptoms can be clearly found in the right half, which visually seems like “fault trajectory” that can be regarded to single-speed fault signatures. The healthy samples are represented by blue points in the lower left corner.

In addition, the experimental results of multi-speed fault diagnosis and 3D fault signatures are summarized in Table III

TABLE 5. Comparative review of related methods and proposed approach for bearing fault diagnosis.

	Abbasian et al. [10]	Paya et al. [11]	Kankar et al. [13]	Lou et al. [14]	Konar et al. [15]	Present Work
Objects	Roller bearings	Bearings and gears	Roller bearings	Ball bearings	Ball bearings	Roller bearings
Defects considered	Bearing looseness, defects in bearing raceways and roller element	Defects on inner race of bearing and gear tooth irregularity	Spall in inner race, outer race, rolling element and combined component defects	Defects on inner race and ball element	Healthy motor and faulty motor with faulted bearing	Defects on inner race, outer race and roller element
Techniques used for fault diagnosis	Meyer wavelet	Daubechies 4	Meyer, Coiflet5, Symlet2, Gaussian, complex Morlet and Shannon wavelets	Daubechies 2 and 10	Morlet and Daubechies 10	Adaptive impulse modelling based wavelet
Features considered	Fundamental cage frequency, inner raceway frequency, outer raceway frequency and ball rotational frequency	10 wavelet numbers indicating both time and frequency and their 10 corresponding amplitudes	Kurtosis, skewness and standard deviation corresponding to scale maximizing energy to Shannon entropy ratio	Standard deviation ratio using the standard deviation as reference	Root mean square (RMS), crest factor and kurtosis	Root mean square (RMS), wavelet power spectrum density (PSD), and kurtosis
Classifier used	Support vector machine	Artificial neural networks	Support vector machines, artificial neural networks, self-organizing maps	Neural fuzzy inference	Support vector machine	Statistical similarity analysis with NN-based classifier using Mahalanobis distance
Classifier efficiencies	100%	96%	98.67%	NA	Wavelet scale: 1-8: 100%; 1-15: 96.67%	100%

and Fig. 8. Different from single-speed result, it can be seen that in Fig. 8 samples representing one condition is consisted with various groups corresponding to the number of rotation speeds used in the training phrase. Interestingly, for both single or multi speed fault signatures, the healthy condition (represented by blue color) intensively locates in the lower left corner with an intensive manner. However, when two rotating speeds of 1000 and 1500 r.p.m used for fault signatures, samples representing roller fault condition (represented by pink color) approximately locate together in feature space. In conclusion, it can be noticed that fault signatures generated using this proposed method can be used to accurately recognize whether the current running state of roller bearing is healthy. Moreover, most of the time, samples would be normally labeled with a certain rotating speed in training phrase. Nevertheless, sometimes it can not achieve high accuracy when the speed of sample can not be tested and determined. In this paper, from Fig. 7 and Fig. 8 it is shown that multi-fault signatures provide a solution that can be used to classify samples to certain groups meanwhile estimate current speed of testing samples by visually comparing with the data distribution plots in feature space dimension.

Additionally, the comparative performance of wavelet analysis using different wavelet kernels was given in Table IV. Each best scale of wavelet transform was selected according to fitness evaluation Eqs. (15), which is used to evaluate the mean statistical similarity between testing samples and given classes. It can be seen that both of IMCWT model and

Daubechies2/4/10 wavelets can achieve 100% classification accuracy; however, misclassified samples occurred when the others used. Moreover, it shows that IMCWT model however enables to obtain the highest trust rate when used for five-speed fault diagnosis compared with the others. In addition, to manifest the efficiency of the proposed approach, recent related diagnostic research work on bearings published in literatures has been reviewed in Table V. In this table, comparison has been conducted based on the perspectives of objects adopted, defects considered, techniques used for fault diagnosis, features considered, classification method used, and the classification efficiencies in each paper.

V. CONCLUSION

In this paper a novel hybrid fault diagnostic method for roller bearing under multi-speed is presented using impulse modelling continuous wavelet transform (IMCWT) model as an advanced signal-processing tool. Particle swarm optimization (PSO) and Broyden-Fletcher-Goldfarb-Shanno (BFGS) based quasi-Newton optimization algorithms are applied to optimize IMCWT model. Nearest neighbor (NN) statistical analysis using Mahalanobis distance is applied as a classifier to map samples into best matching classes.

In this proposed approach, IMCWT can be effectively applied to extract fault information from vibration signals by means of providing high time-frequency resolution for signal analysis. Reduced three-dimensional feature space dimension (i.e., RMS, PSD, and kurtosis) is adopted to

extract fault features after wavelet decomposition. After that, NN-based classifier and Mahalanobis vector distance are used to evaluate vector similarity between samples to be labeled and given classes for identifying conditions of testing samples. At last, the effectiveness of this proposed method is verified and presented.

An overall accuracy of 100% was achieved in the experimental results, which demonstrated that this proposed approach can be used to effectively classify vibration signals of four conditions of roller bearing, i.e., normal, with the fault of inner race, outer race, and roller operation. In addition, it can be easily seen that this method meanwhile provides discriminatory fault signatures for both single-speed and multi-speed data sets, which has great scope for extending this technique in identifying other types of rotating mechanical faults.

This proposed approach is simple and easy to implement providing a feasible method for multi-speed fault diagnosis of roller bearing in rotating machinery. Hence, in the future this method would be further extended to diagnose other rotating components in industrial plants.

REFERENCES

- [1] J. Chen *et al.*, "Wavelet transform based on inner product in fault diagnosis of rotating machinery: A review," *Mech. Syst. Signal Process.*, vol. 70, pp. 1–35, Sep. 2016.
- [2] J. Huang, G. Chen, L. Shu, S. Wang, and Y. Zhang, "An experimental study of clogging fault diagnosis in heat exchangers based on vibration signals," *IEEE Access*, vol. 4, pp. 1800–1809, Jun. 2016.
- [3] P. J. Tavner, "Review of condition monitoring of rotating electrical machines," *IET Electr. Power Appl.*, vol. 2, no. 4, pp. 215–247, Jul. 2008.
- [4] M. A. Abu-Zeid and S. Abdel-Rahman, "Bearing problems' effects on the dynamic performance of pumping stations," *Alexandria Eng. J.*, vol. 52, no. 3, pp. 241–248, 2013.
- [5] M. Kang, M. R. Islam, J. Kim, J.-M. Kim, and M. Pecht, "A hybrid feature selection scheme for reducing diagnostic performance deterioration caused by outliers in data-driven diagnostics," *IEEE Trans. Ind. Electron.*, vol. 63, no. 5, pp. 3299–3310, May 2016.
- [6] B. Kim, S. Lee, M. Lee, J. Ni, J. Song, and C. Lee, "A comparative study on damage detection in speed-up and coast-down process of grinding spindle-typed rotor-bearing system," *J. Mater. Process. Technol.*, vol. 187, pp. 30–36, Oct. 2007.
- [7] T. Christopher and G. P. Compo, "A practical guide to wavelet analysis," *Bull. Amer. Meteorol. Soc.*, vol. 79, no. 1, pp. 61–78, 1998.
- [8] M. M. Tahir, A. Q. Khan, N. Iqbal, A. Hussain, and S. Badshah, "Enhancing fault classification accuracy of ball bearing using central tendency based time domain features," *IEEE Access*, vol. 5, pp. 72–83, 2017.
- [9] H. Hong and M. Liang, "Fault severity assessment for rolling element bearings using the Lempel–Ziv complexity and continuous wavelet transform," *J. Sound Vibrat.*, vol. 320, no. 1, pp. 452–468, 2009.
- [10] S. Abbasion, A. Rafsanjani, A. Farshidianfar, and N. Irani, "Rolling element bearings multi-fault classification based on the wavelet denoising and support vector machine," *Mech. Syst. Signal Process.*, vol. 21, no. 7, pp. 2933–2945, Sep. 2007.
- [11] B. Paya, I. Esat, and M. Badi, "Artificial neural network based fault diagnostics of rotating machinery using wavelet transforms as a preprocessor," *Mech. Syst. Signal Process.*, vol. 11, no. 5, pp. 751–765, 1997.
- [12] J. Zarei, M. A. Tajeddini, and H. R. Karimi, "Vibration analysis for bearing fault detection and classification using an intelligent filter," *Mechatronics*, vol. 24, no. 2, pp. 151–157, 2014.
- [13] P. Kankar, S. C. Sharma, and S. Harsha, "Fault diagnosis of ball bearings using continuous wavelet transform," *Appl. Soft Comput.*, vol. 11, no. 2, pp. 2300–2312, 2011.
- [14] X. Lou and K. A. Loparo, "Bearing fault diagnosis based on wavelet transform and fuzzy inference," *Mech. Syst. Signal Process.*, vol. 18, no. 5, pp. 1077–1095, Sep. 2004.
- [15] P. Konar and P. Chattopadhyay, "Bearing fault detection of induction motor using wavelet and support vector machines (SVMs)," *Appl. Soft Comput.*, vol. 11, no. 6, pp. 4203–4211, 2011.
- [16] E. Schukin, R. Zamaraev, and L. Schukin, "The optimisation of wavelet transform for the impulse analysis in vibration signals," *Mech. Syst. Signal Process.*, vol. 18, no. 6, pp. 1315–1333, 2004.
- [17] J. Kennedy, "Particle swarm optimization," in *Encyclopedia of Machine Learning*. New York, NY, USA: Springer, 2011, pp. 760–766.
- [18] R. Battiti and F. Masulli, "BFGS optimization for faster and automated supervised learning," in *Proc. Int. Neural Netw. Conf.* 1990, pp. 757–760.
- [19] D. Dyer and R. Stewart, "Detection of rolling element bearing damage by statistical vibration analysis," *J. Mech. Design*, vol. 100, no. 2, pp. 229–235, 1978.
- [20] A. Nabhan, M. Nouby, A. Sami, and M. Mousa, "Multiple defects detection in outer race of gearbox ball bearing using time domain statistical parameters," *Int. J. Vehicle Struct. Syst.*, vol. 8, no. 3, p. 167, 2016.
- [21] Y. Wang, J. Xiang, R. Markert, and M. Liang, "Spectral kurtosis for fault detection, diagnosis and prognostics of rotating machines: A review with applications," *Mech. Syst. Signal Process.*, vol. 66, pp. 679–698, Sep. 2016.
- [22] J. Tian, C. Morillo, M. H. Azarian, and M. Pecht, "Motor bearing fault detection using spectral kurtosis-based feature extraction coupled with k-nearest neighbor distance analysis," *IEEE Trans. Ind. Electron.*, vol. 63, no. 3, pp. 1793–1803, Mar. 2016.
- [23] J. Cusidócusido, L. Romeral, J. A. Ortega, J. A. Rosero, and A. G. Espinosa, "Fault detection in induction machines using power spectral density in wavelet decomposition," *IEEE Trans. Ind. Electron.*, vol. 55, no. 2, pp. 633–643, Feb. 2008.
- [24] T. Cover and P. Hart, "Nearest neighbor pattern classification," *IEEE Trans. Inf. Theory*, vol. 13, no. 1, pp. 21–27, Jan. 1967.
- [25] Z. Hu, M. Xiao, L. Zhang, S. Liu, and Y. Ge, "Mahalanobis distance based approach for anomaly detection of analog filters using frequency features and Parzen window density estimation," *J. Electron. Test.*, vol. 32, no. 6, pp. 681–693, 2016.
- [26] *PT 500 Machinery Diagnostic System*, accessed Dec. 9, 2016. [Online]. Available: http://www.gunt.de/static/s3680_1.php



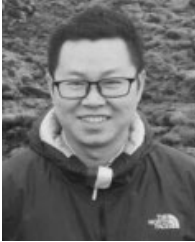
ZHIQIANG HUO received the B.S. and M.S. degrees from the China University of Geosciences Beijing, China, in 2013 and 2016, respectively. He is currently pursuing the Ph.D. degree with the University of Lincoln, U.K. His field of interest is mechanical fault diagnosis, mobile crowdsensing, and middleware in wireless sensor networks.



YU ZHANG received the B.Sc. degree from the School of Aerospace Engineering and Applied mechanics, Tongji University, Shanghai, China, in 2004, and the M.Sc. degree and Ph.D. degree from the Department of Civil Engineering, University of Nottingham, Nottingham, U.K. in 2005 and 2011, respectively. She is currently a Senior Lecturer with the School of Engineering, University of Lincoln, Lincoln, U.K. Her research interests include equipment fault detection and diagnosis, grey-box system modeling, and development of data analysis and machine learning algorithms. Her recent major projects, including two Innovate U.K projects, one international project with the Guangdong University of Petrochemical Technology and one industrial project funded by Siemens, Germany, all focus on the areas of data analysis and machine fault diagnosis.



PIERRE FRANcq received the B.S. degree from the University of Toulouse, France, in 2015. He is currently pursuing the M.S. degree in engineering with the Mines Albi, University of Toulouse. His fields of interest are supply chain management, lean management, and nonlinear programming.



LEI SHU is currently a Lincoln Professor with the University of Lincoln, U.K., and a Distinguished Professor with the Guangdong University of Petrochemical Technology. He is also the Executive Director of the Guangdong Provincial Key Laboratory of Petrochemical Equipment Fault Diagnosis, China. He has authored or co-authored over 300 papers in related conferences, journals, and books in the area of sensor networks. His main research field is wireless sensor networks. He received the

Globecom in 2010 and the ICC 2013 Best Paper Award. He has been serving as the Editor-in-Chief of the EAI Endorsed Transactions on Industrial Networks and Intelligent Systems, and as an Associate Editor of the IEEE Systems Journal, the IEEE Access, and so on. He has served as over 50 various Co-Chair for international conferences/workshops, including the IWCMC, the ICC, the ISCC, the ICNC, the Chinacom, especially, a Symposium Co-Chair of the IWCMC in 2012, the ICC in 2012, a General Co-Chair of the Chinacom in 2014, the Qshine in 2015, the Collaboratecom in 2017, the Mobiquitous in 2018, the Steering and TPC Chair of the InisCom in 2015, a TPC Member of over 150 conferences, including, the ICDCS, the DCOSS, the MASS, the ICC, the Globecom, the ICCCN, the WCNC, and the ISCC.



JIANFENG HUANG (M'15) received the Ph.D. degree from the South China University of Technology, Guangzhou, China, in 2016. He currently with the Guangdong University of Petrochemical Technology as an Associate Professor and the Department Head of Safety Engineering. Since 2012, he has been with the Guangdong Petrochemical Equipment Fault Diagnosis Key Laboratory. His research interests include industrial wireless sensor networks, petrochemical equipment fault diagnosis, and safety assessment.

• • •